How to obtain Pt(IV) complexes suitable for the conjugation to nanovectors from the oxidation of [PtCl(terpyridine)]$^+$.

E. Gabano,[a] E. Perin,[a] C. Fielden,[b] J. A. Platts,[b] A. Gallina,[a] B. Rangone,[a] M. Ravera.[a,*]

Oxidation of [Pt$^{(II)}$Cl(terpy)]$^+$ (terpy = 2,2':6',2"-terpyridine) has been attempted with several oxidizing agents and in different experimental conditions in order to obtain a Pt(IV) complex suitable for the conjugation to nanovectors to be used in drug delivery targeting for anticancer therapy. The best compromise in terms of yield and purity of the final complex was obtained by microwave-assisted reaction at 70 °C in 50% aqueous H_2O_2 for 2 h. Under these conditions the quantitative formation of [Pt$^{(IV)}$Cl(OH)$_2$(terpy)]$^+$ was observed. Subsequent synthetic steps were *i)* functionalization of [Pt$^{(IV)}$Cl(OH)$_2$(terpy)]$^+$ in the axial position with succinic anhydride to obtain [Pt$^{(IV)}$Cl(OH)(succinato)(terpy)]$^+$, and *ii)* reaction of the latter with nonporous silica nanoparticles (SNPs) with an external shell containing primary amino groups to obtain a nanovector able to transport the Pt(IV) antitumor prodrug in form of conjugate Pt-SNP. Finally, the antiproliferative activity and cell accumulation of [Pt$^{(II)}$Cl(terpy)]$^+$, [Pt$^{(IV)}$Cl(OH)$_2$(terpy)]$^+$, and Pt-SNP conjugate were measured on three cancer cell lines. Despite highly effective accumulation of Pt-SNP into cells, a modest increase in activity was observed with respect to the molecular species. Further experiments showed that the Pt-SNP conjugate can release [Pt$^{(II)}$Cl(terpy)]$^+$ upon reduction, but this metabolite may undergo hydrolysis, and the resulting aquo complex could coordinate once again the free amino groups of the SNPs. In the resulting tetraamine form, the Pt(II) complex conjugated to the SNPs cannot completely exert its antiproliferative activity.

Introduction

The traditional structure-activity relationship (SAR) rules for antitumor Pt(II) complexes indicated that triamine compounds are scarcely cytotoxic.[1-3] In fact most of these complexes have very low potency because, in contrast to Pt-diamine compounds like cisplatin (*cis*-[PtCl$_2$(NH$_3$)$_2$]), they can only bind DNA in a monofunctional way.[4] However, some *cis*-[Pt(A)(Cl)(NH$_3$)$_2$]$^+$ cations, where A is a derivative of pyridine, pyrimidine, purine, or aniline, inhibit DNA synthesis, block DNA polymerases and are active against *in vivo* tumor models.[5, 6] In particular, transcription is strongly inhibited by *cis*-[PtCl(NH$_3$)$_2$(py)]$^+$ (py = pyridine), whereas adducts of [PtCl(dien)]$^+$ (dien = diethylenetriamine), which do not have the same steric hindrance, are less effective. Although the block of transcription by cisplatin and *cis*-[PtCl(NH$_3$)$_2$(py)]$^+$ is similar, repair of adducts formed by the latter is reduced so that they persist longer than those of cisplatin,[7] and the activity of triamine complexes seems to be related to their steric hindrance.[8] Moreover, Lippard *et al.* showed that, among several monofunctional platinum(II) complexes, phenanthriplatin (*cis*-[PtCl(NH$_3$)$_2$(phenanthridine)]$^+$) displays significant antitumor properties. Its cellular response is different from cisplatin-like drugs because DNA intercalation is associated with monodentate binding. The resulting adducts inhibit transcription, whereas the low distortion of DNA significantly eludes repair. Thus, phenanthriplatin proved to be very effective on several cell lines.[9-15]

Recently, triamine (or in general monofunctional) Pt(II) complexes have been re-evaluated as anticancer drugs,[16] since carefully designed ligands allow the resulting Pt compounds to bind with DNA in a different manner. This could result in alternative cell death mechanisms and/or circumvention of Pt resistance. In particular, Pt(II) complexes containing terpyridine (terpy = 2,2':6',2"-terpyridine) derivatives, that can be regarded as quite bulky triamine complexes,[17] are interesting since some can intercalate into the DNA duplex, with a preference for 5'-CG sites, due to greater polarity compared to A-T base pairs.[18, 19] The Pt(II)-terpy complexes also interact with four-stranded G-quadruplex DNA.[20-24] G-quadruplex emerged as a promising anti-cancer target because their stabilization indirectly inhibits the telomerase enzyme. This enzyme is expressed in more than 85% of human tumors and compensates the loss of telomeres at each round of replication, thus contributing to cancer survival.[25, 26] In another scenario, Pt(II)-terpy complexes were found to inhibit the growth of different morphological forms of *Trypanosoma cruzi* and *Trypanosoma brucei*, the parasitic protozoa causative agents of Chagas' disease and African trypanosomiasis (sleeping sickness), respectively.[27, 28] Finally, Pt(II)-terpy derivatives with luminescence properties have been studied for bioimaging as DNA staining agents[29] and biotinylated Pt(II)-ferrocenylterpyridine complexes were also tested for targeted photoinduced cytotoxicity.[30]

A strategy to reduce toxicity and improve uptake properties of antitumor Pt complexes is to turn them into Pt(IV) prodrugs. Such complexes can be reduced in the hypoxic tumor environment to the corresponding cytotoxic Pt(II) metabolite with loss of axial ligands (*activation by reduction*). The saturated six-coordinated octahedral geometry of Pt(IV) is generally characterized by kinetic inertness that minimizes off-target effects, thus improving the therapeutic properties and allowing oral administration.[31-34] In this context, it is interesting to study Pt(IV) derivatives of Pt(II)-terpy cations, since only few such derivatives have been already reported, where the Pt(II) precursor was oxidized with Cl_2,[35] or [KAuCl$_4$].[36]

A further possibility to improve the activity of a drug is the exploitation of drug targeting and delivery (DTD) methods. Active DTD uses specific molecular interactions between the

[a] *Dipartimento di Scienze e Innovazione Tecnologica, Università del Piemonte Orientale, Viale Michel 11, 15121 Alessandria (Italy)*
[b] *School of Chemistry, Cardiff University, Park Place, Cardiff CF10 3AT (UK).*
*Electronic Supplementary Information (ESI) available: NMR and ESI-MS characterization of compounds **2** and **3**.*

drugs and cancer cell or tissue. On the contrary, passive DTD takes advantage of the enhanced permeability and retention (EPR) effect in tumor tissues, by using functionalized polymers, nanoparticles, micelles, liposomes or nanotubes and their conjugation with the drugs.[37] By this effect, macromolecules selectively gather in the tumor interstice, because the tumor vessels are highly disordered and swollen with abundant pores resulting in enlarged gap junctions between endothelial cells and compromised lymphatic drainage.[37] Recently, amino-functionalized silica nanoparticles (NPs) were tested as efficient carriers for Pt(IV) prodrugs. Controlled drug release from NPs exploits the combination between the unique features of the Pt(IV) prodrugs and those of the tumor environment. The *in vitro*/*in vivo* activation by reduction of the Pt(IV) moiety releases the active square planar Pt(II) metabolite, with consequent detachment of the axial ligand/s bearing the vector/s.[34, 38, 39]

In this paper, the synthesis, characterization and *in vitro* evaluation of Pt(IV)-terpy complexes (Fig. 1) and the corresponding SNPs conjugate are described. Interestingly, most of the traditional synthetic methods failed to give the desired intermediates and microwave-assisted reactions[40] had to be performed. Such behavior was also theoretically investigated with DFT calculations.

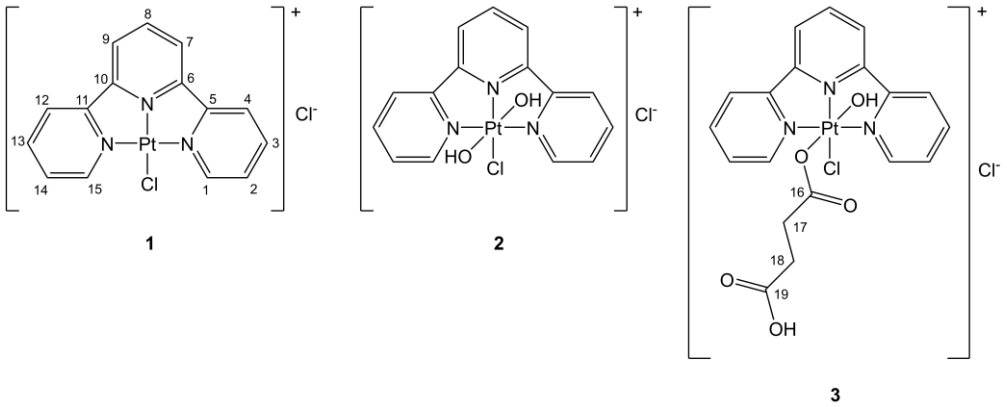

Fig. 1. Sketch of the synthesized complexes **1**-**3** with numbering scheme for the assignment of NMR signals.

Results and discussion

Synthesis of Pt(IV) complexes containing terpyridine.

Complex **1** was synthesized from [$PtCl_2(\eta^4$-cod)] (cod = cycloocta-1,5-diene) and terpy according to literature procedures (see experimental section for details).[24, 41, 42] The following step of oxidation of complex **1** was performed with several oxidizing agents in order to prepare different Pt(IV) synthons, potentially useful for further coupling reactions (Scheme 1).[36, 43-48] Surprisingly, the most common reaction conditions failed to get the expected final products. Iodobenzene dichloride[36] and *N*-chlorosuccinimide[45] with both traditional and microwave-assisted heating gave no oxidation at all. The use of peroxyacetic acid led to the formation of up to 5% of the acetato-hydroxido Pt(IV) product **2A**. Only H_2O_2 was efficient in oxidizing complex **1**, but the results were strongly dependent on the reaction conditions. When hydrogen peroxide and acetonitrile were used to generate the reactive peroxyacetimidic acid,[46, 47] only 12% oxidation of **1**, to obtain the acetylamido-hydroxido Pt(IV) complex **2B**, was observed. Syntheses in ethanol with large excess H_2O_2 to get the ethoxido-hydroxido derivative **2C** gave no reaction with traditional heating and only up to 15% of oxidized product with microwave heating. When acetic acid was used as a solvent, H_2O_2 was partially successful to give **2A**. Traditional heating (at 30 °C or 50 °C) with 50:1 excess 50% aqueous H_2O_2 from 1.5 to 48 h gave up to 50% of oxidized product in the milder conditions, whereas high temperature for a long time led to about 15% of the diacetato product **2D**. On the contrary, the microwave-assisted synthesis gave **2A** by heating **1** at 70 °C for 5 min with 50:1 excess 50% aqueous H_2O_2. Under these conditions, 50% of **1** was oxidized, and this value did not significantly increase by increasing both excess H_2O_2 and/or reaction time.

As **2A** was the most successful derivative at this stage of the work, its purification was attempted. The chloride counter ion was exchanged with hexafluorophosphate by using an anion exchange resin to more easily precipitate it. A further step on resin was used to re-introduce chloride counter ions to gain in water solubility. However, the final product did not reach purity higher than 70%, and, for this reason, **2A** was abandoned.

When water was used as a solvent, neither mild (*i.e.* room temperature, 5:1 excess 35% aqueous H_2O_2, overnight) nor strong (*i.e.* 70 °C, 22:1 excess 35% aqueous H_2O_2, overnight) traditional methods resulted in oxidation of **1**.[43, 44] On the contrary, microwave-assisted reaction at 70 °C in 50% aqueous H_2O_2 for 2 h was successful in the quantitative formation of **2** (see experimental section for details). For this reason, **2** was the chosen intermediate for the following work.

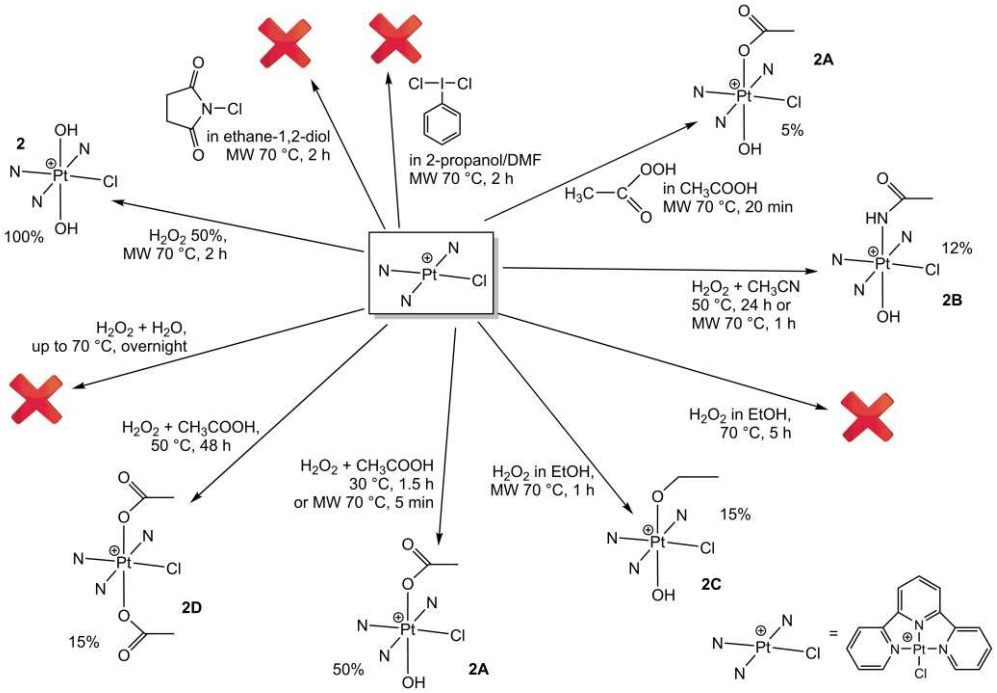

Scheme 1. Summary of the attempted oxidation reactions of **1**. The heating was performed with traditional hot plates, except where otherwise indicated (MW = microwave).

DFT Calculations

The enthalpy change for reaction "$Pt^{(II)}$" + $H_2O_2 \rightarrow$ "$Pt^{(IV)}(OH)_2$" was calculated in the case of cisplatin and complex **1**. Two other complexes were added in the calculations, i.e. [$PtCl_2$(dach)] (dach = cyclohexane-1*R*,2*R*-diamine) and $[PtCl(dien)]^+$, for comparison with "$PtCl_2N_2$" and "$PtClN_3$" containing an aliphatic chelating ligands. DFT calculations (see experimental section for details) predict similar values for cisplatin, [$PtCl_2$(dach)] and $[PtCl(dien)]^+$ (ΔH = -170, -194 and -184 kJ mol^{-1}, respectively), but a much smaller negative ΔH for **1** (-92 kJ mol^{-1}). These data support the lower reactivity of **1** with hydrogen peroxide. On the contrary, [$PtCl_2$(dach)] is usually oxidized in the same conditions of cisplatin[44, 49] and $[PtCl(dien)]^+$ can be easily oxidized with 5:1 excess 35% aqueous H_2O_2 at room temperature overnight (50% of oxidized product). To seek explanation for this behaviour, frontier orbitals were examined (Fig. 2): comparison of **1** with $[PtCl(dien)]^+$ shows that HOMOs are similar in form and energy, but that the LUMO of **1** is delocalized over the terpy ligand, with very little density at Pt and none in the Pt—Cl bond, unlike in $[PtCl(dien)]^+$ where the LUMO has large contributions from Pt d-orbital and the Pt—Cl bond.

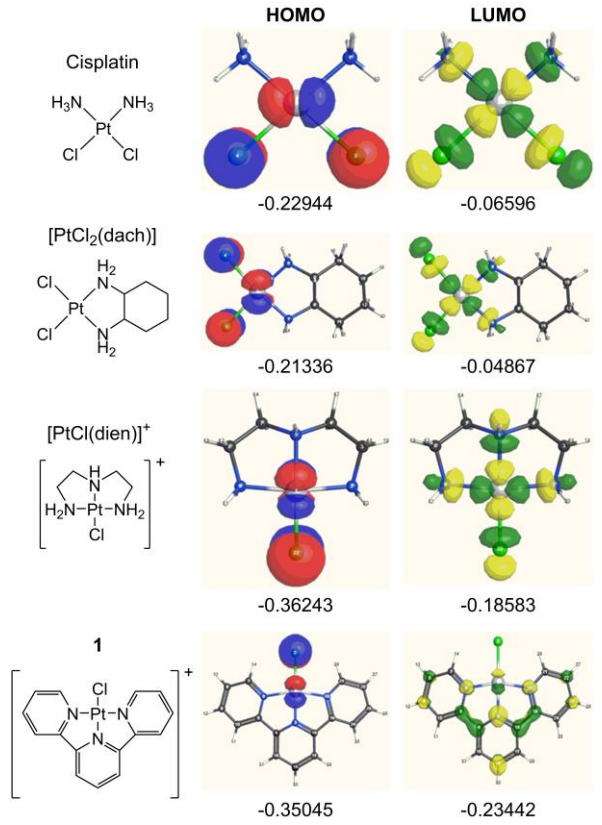

Fig. 2. HOMO and LUMO energies (au) and isosurface plots (at 0.04 au level) for cisplatin, [$PtCl_2$(dach)], $[PtCl(dien)]^+$ and **1**.

Functionalization of 2 in the axial position and coupling with silica nanoparticles

A subsequent synthetic step consisted of functionalization of **2** in the axial position/s. Succinic and glutaric anhydrides were chosen to introduce a linker necessary for further reaction with DTD vectors. These anhydrides generate two carboxylic groups, one of which reacts with an axial OH of **2**, and the other one remaining free for further conjugation. A 5:1 excess of succinic or glutaric anhydride (70 °C, overnight in DMF) gave no substitution reactions on **2**, but caused its reduction to **1**. A decrease in temperature (40 °C) led to different results: with glutaric anhydride, 15% of monoglutarato Pt(IV) product was obtained, together with partial reduction of **2**, whereas with succinic anhydride 75% of monosuccinato complex **3** was obtained (see experimental section for details). As **3** gave the best compromise in terms of yield and purity, the final step was limited to it.

Nonporous silica nanoparticles (SNPs) with an external shell containing primary amino groups were chosen as DTD vector to transport the Pt(IV) antitumor prodrug. Silica nanoparticles have attracted significant interest because of their acceptable biocompatibility, low cost large-scale synthesis, easy control of surface properties, and the possibility to modify the external shell with chemical functionalities needed to introduce the Pt(IV) moiety. Spherical SNPs containing the 3-aminopropyl arm were produced according to literature methods (relevant features: amino group density = 0.283 mmol NH_2 g^{-1} SNPs, dynamic light scattering diameter = 125±2 nm, ζ potential = 53±2 mV).[39] The SNPs were loaded with **3**, after activation of the pendant carboxylic group with the common EDC/NHS (EDC = *N*-(3-dimethylaminopropyl)-*N'*-ethylcarbodiimide, NHS = *N*-hydroxysuccinimide) coupling strategy, through the formation of amide bonds to form conjugate **4**. The Pt content in **4** was evaluated by inductively coupled plasma optical emission spectroscopy (ICP-OES) and the results indicated about 2% of coupling, *i.e.* 6.1 μmol Pt g^{-1} SNPs. The complete series of reactions from **1** to **4** is reported in Scheme 2.

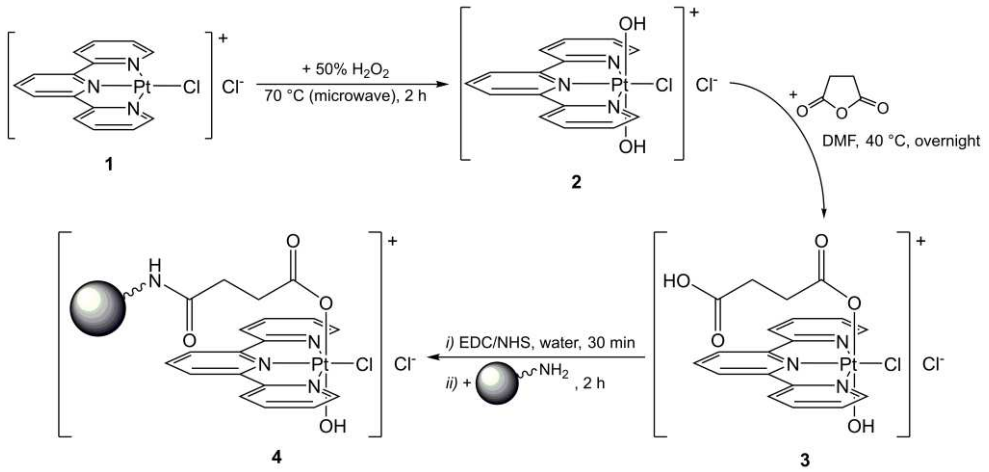

Scheme 2. Sketch of the complete series of reactions from **1** to **4**. EDC = N-(3-dimethylaminopropyl)-N'-ethylcarbodiimide, NHS = N-hydroxysuccinimide; grey balls represent amino-functionalized nonporous silica nanoparticles (SNPs).

***In vitro* tests**

Compounds 1, 2 and 4 were tested on human ovarian cancer cells A2780 and two cell lines derived from human malignant pleural mesothelioma (MPM), a very difficult to treat tumor (sarcomatoid MM98 cell line and its cisplatin-resistant MM98R subline). The reference drug cisplatin was added for comparison purposes. The results are reported in Table 1 and Fig. 3.

Table 1. Cytotoxicity (IC_{50}), resistance factor (RF), and accumulation ratio (AR) measured for cisplatin, compounds **1** and **2**, and conjugate **4**, respectively. Data are means ± standard deviations of at least three independent replicates.

Compounds	IC_{50} [μM][a]			RF[c]	AR[d]	
	A2780	MM98	MM98R		A2780	MM98
Cisplatin	0.5± 0.1[b]	3.2 ± 1.0[b]	19.4 ± 2.8[b]	6.1	1.4 ± 0.6[e]	2.71±0.18
1	2.80±0.25	5.41±2.09	4.11±0.66	0.76	0.34±0.03	0.43±0.13
2	7.01±0.56	10.5±0.1	8.09±0.91	0.77	0.86±0.69	0.17±0.05
4	0.74±0.05	4.53±0.45	5.78±0.74	1.3	36.9±14.9	57.8±4.5

[a] IC_{50} data were obtained after 72 h of treatment of A2780 ovarian cancer, MM98 malignant pleural mesothelioma and its cisplatin resistant subline MM98R cells; [b] from ref. [50]; [c] RF = IC_{50} (MM98R) / IC_{50} (MM98); AR = ratio between the intracellular and the extracellular Pt concentration (cells were treated for 4 h with 10 μM Pt concentrations); [e] from ref. [51].

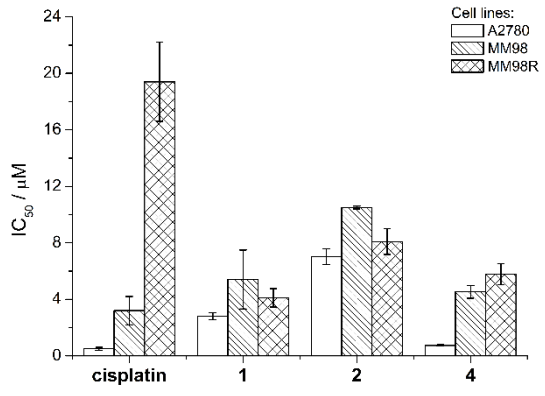

Fig. 3. Comparison between IC_{50} values of cisplatin, compounds **1** and **2**, and conjugate **4**. See Table 1 for details.

The Pt(II) precursor **1** was less active than cisplatin except for the cisplatin-resistant MM98R cells, where it maintained about the same activity shown on sensitive MM98 cells (see resistance factor, RF, *i.e.* the ratio between IC_{50} on MM98R and MM98, respectively). In the oxidized form **2** the activity was uniformly lowered. In the case of the conjugate **4**, the activity on A2780 cells was only 4 times better than that of **1** and almost the same on MM98 and MM98R cells. Cellular accumulation of all four compounds was evaluated by means of the intracellular Pt content after 4 h of treatment and expressed as accumulation ratio (AR, *i.e.* the ratio between the intracellular and the extracellular Pt concentration). The results in Table 1 show that the SNPs are highly effective for accumulation of Pt into cells (more than 100 times increase in AR from **1** to **4**).[38, 39] These data would suggest an increase in activity from **1** to **4** that, surprisingly, does not occur.

In the attempt to explain these results, the solution behavior and reduction properties of **1** and **3** (*i.e.* the Pt(II) precursor and the complex conjugated to the SNPs, respectively) were investigated. The stability in solution of **1** and **3** was studied in HEPES buffer (HEPES = 4-(2-hydroxyethyl)-1-piperazineethanesulfonic acid, pH = 7.5) at 37 °C with HPLC-MS technique. **1** easily underwent hydrolysis with the loss of one chloride (about 50% decrease of peak area of **1** in 15 min)[17] and this is in agreement with the previously reported propensity to the loss of the ligand *trans* to terpy in this kind of complexes.[27] On the contrary, **3** was hydrolyzed with the loss of the succinato ligand in longer times (about 50% decrease of peak area of **3** in 24 h). **3** was also reacted with a 10-fold excess of ascorbic acid, as the simplest model of bio-reductant, in HEPES buffer. The results indicated that **3** is easily reduced (about 50% of peak area decrease in 20 min); this data is consistent with the difficulties in the oxidation of **1** and in the synthesis of **3** often accompanied by reduction.

The fast reduction of **3** should guarantee the release of the Pt(II) metabolite from the conjugate **4**. However, AR data showed high accumulation of Pt due to the endocytosis of **4** without the expected corresponding increase in activity with respect to **1**. The propensity to hydrolysis of **1**, *i.e.* the Pt(II) metabolite of **4**, could explain such strange behavior. Therefore, to unravel the mystery, complex **1** was dissolved and maintained for 4 h in an aqueous suspension of the SNPs. After washing and mineralization, the Pt content on the SNPs was measured, resulting in the conjugation of 3.9% of the total available amino groups (11.0 μmol Pt g^{-1} SNPs). The data support the hypothesis that conjugate **4** may release **1** upon reduction *in vitro*. After hydrolysis, the aquo derivative of **1** (i.e. $[Pt(H_2O)(terpy)]^{2+}$) could "re-coordinate" the free amino groups of the SNPs, and, in turn, it can be retained, at least in part, by the nanoparticles as Pt(II) complex. In the resulting tetraamine form, the Pt(II) complex conjugated to the SNPs is no longer able to exert its antiproliferative activity. Furthermore, even though the *trans* orienting effect of terpy could, at least in part, cause the release of hydrolyzed **1** from the amine-decorated nanoparticles, this complex can re-coordinate the SNPs again.

Experimental section

General procedures

$K_2[PtCl_4]$ (Johnson Matthey and Co.) and all other chemicals (Sigma Aldrich) were used without further purification. Water was purified (18 MΩ cm) using a standard Milli-Q system (Millipore, Bedford, MA, USA).

The reactions under microwave irradiation were performed by using a CEM Discover® SP System equipped with a focused single mode and self-tuning cavity, an air cooling system, an automated power control based on temperature feedback, supplying power in 1 W increments from 0 to 300 W.

The NMR spectra were measured on a NMR-Bruker Avance III spectrometer operating at 500 MHz (^{1}H), 125.7 MHz (^{13}C) and 107.2 MHz (^{195}Pt with a spectral window of 2000 ppm), respectively, and a JEOL Eclipse Plus spectrometer operating at 400 MHz (^{1}H), 100.6 MHz (^{13}C) and 86.0 MHz (^{195}Pt, with a spectral window of 2000 ppm), respectively. ^{1}H and ^{13}C NMR chemical shifts were reported in parts per million (ppm) referenced to solvent resonances. ^{195}Pt NMR spectra were recorded using a solution of K_2PtCl_4 in saturated aqueous KCl as the external reference. The shift for K_2PtCl_4 was adjusted to -1628 ppm from Na_2PtCl_6 (δ = 0 ppm).

RP-HPLC and mass analysis were performed using a Waters HPLC-MS instrument equipped with Alliance 2695 separations module, 2487 dual lambda absorbance detector and 3100 mass detector. Chromatographic analyses were carried out using a C18 Phenomenex Phenosphere-NEXT (5-μm, 250×4.6 mm ID) column. The mobile phase employed was a 70/30 (for **1** and **2**) or 90/10 (for **3**) mixture of 15mM formic acid / methanol; the flow rate was 0.5 mL/min and the UV-visible detector was set at 210 nm. Electrospray ionization mass spectra (ESI-MS) were obtained setting the source and desolvation temperatures to 150 °C and 250 °C, respectively, and using nitrogen both as a drying and as a nebulizing gas. The cone and the capillary voltages were usually 30 V or 20 V and 2.70 kV, respectively. Quasi-molecular ion peaks $[M+H]^+$ or $[M-H]^-$ peaks were assigned on the basis of the *m/z* values and of the simulated isotope distribution patterns.

Mineralization of Pt-loaded SNPs was performed using a microwave-assisted acid digestion apparatus Milestone Start D (Milestone Srl, Sorisole, Italy) with internal temperature sensor. Platinum was quantified by inductively coupled plasma-optical emission spectrometry (ICP-OES, Spectro Genesis, Spectro Analytical Instruments, Kleve, Germany) equipped with a crossflow nebulizer, or by inductively coupled plasma-mass spectrometry (ICP-MS, Thermo Optek X Series 2). A platinum standard stock solution of 1000 mg L^{-1} was diluted in 1.0% v/v nitric acid to prepare calibration standards. To quantify the platinum concentration by ICP-OES, the Pt 299.797 nm line was selected. Instrumental settings for ICP-MS were optimized to yield maximum sensitivity for platinum. For quantitative determination, the most abundant isotopes of platinum and indium (used as internal standard) were measured at *m/z* 195 and 115, respectively.

Synthesis of (*SP*-4-2)-dichlorido(cycloocta-1,5-diene)platinum(II), [$PtCl_2$(cod)]

[$PtCl_2$(cod)] was synthesized according to literature procedures.[24, 41] In particular, potassium tetrachloroplatinate(II) (1.00 g, 2.41 mmol) was dissolved in 16 mL of ultrapure water and the red solution was filtered to remove possible solid residues. Then, 24 mL of glacial acetic acid and cycloocta-1,5-diene (1.00 mL, 8.15 mmol) were added and the mixture was magnetically stirred for 2 h at 90 °C, in the dark. During this time, the solution turned from red to pale yellow and a white solid precipitated. When significant changes were no longer observed, three quarter of the solvent was removed under reduced pressure and the white solid was separated by centrifugation, washed with ultrapure water, ethanol and diethyl ether and then dried *in vacuo*. Yield: 703 mg, 1.88 mmol, 78.0%. ^{1}H-NMR (500 MHz, $CDCl_3$), δ: 2.27 and 2.71 (m, 8H, -CH_2), 5.61 (m, 4H, -C*H*) ppm. ^{13}C-NMR (500 MHz, $CDCl_3$), δ: 31.0 (-*C*H_2), 100.2 (-*C*H) ppm. ^{195}Pt-NMR (500 MHz, $CDCl_3$), δ: -3342 ppm.

Synthesis of (*SP*-4-2)-chlorido(2,2':6',2''-terpyridine)platinum(II) chloride (1)

Complex **1** was synthesized according to literature procedures.[42] Briefly, [$PtCl_2$(cod)] (154 mg, 0.412 mmol) was suspended in 10 mL of ultrapure water. Then, terpy (101 mg, 0.433 mmol) was added to the mixture, which was magnetically stirred for 30 min at 70 °C. The red mixture was dried under reduced pressure and the red residue was washed with diethyl ether and then dried *in vacuo*. Yield: 170 mg, 0.341 mmol, 82.7%. ^{1}H-NMR (400 MHz, MeOD-d_4), δ: 7.79 (m, H2, H14, 2H), 8.40 (m, H1, H15, H3, H13, H7, H9, 6H), 8.47 (m, H8, 1H), 8.82 (m, H4, H12, 2H) ppm. ^{13}C-NMR (100.6 MHz, MeOD-d_4), δ: 124.1 (C1, C15), 125.3 (C7, C9), 128.7 (C2, C14), 141.7 (C8), 142.4 (C3, C13), 151.4 (C4, C12), 154.9 (C5, C11), 158.8 (C6, C10) ppm. ^{195}Pt-NMR (86.0 MHz, MeOD-d_4), δ: -2734 ppm. ESI-MS: calcd for $C_{15}H_{11}Cl_2N_3Pt$ [M] 499 m/z, found (positive ion mode) 464 m/z $[M\text{-}Cl]^+$.

Synthesis of (*OC*-6-32)-chloridodihydroxido(2,2':6',2''-terpyridine)platinum(IV) chloride (2)

Complex **1** (40.0 mg, 0.0801 mmol) was dissolved in 50% w/w aqueous hydrogen peroxide (2.00 mL, 35.2 mmol) in a microwave vessel. The vessel was capped and introduced into the microwave cavity. The microwave unit heated the vessel content to 70 °C over a 5-min ramp period and then maintained this temperature for 2 h while stirring the mixture with a magnetic bar; the power was automatically set at 50 W. After heating, the vessel was allowed to cool to room temperature before removing it from the cavity. The solvent was removed under reduced pressure and the addition of acetone/diethyl ether allowed one to get a yellow solid, that was washed with diethyl ether and then dried *in vacuo*. Yield: 35.0 mg, 0.0656 mmol, 81.9%. ^{1}H-NMR (500 MHz, D_2O), δ: 8.16 (t, H2, H14, 2H, ^3J = 6.7 Hz), 8.64 (t, H3, H13, 2H, ^3J = 7.8 Hz), 8.73 (d, H7, H9, 2H, ^3J = 7.8 Hz), 8.81 (s, H1, H8, H15, 3H), 9.35 (d, H4, H12, 2H, ^3J = 5.6 Hz) ppm. ^{13}C-NMR (125.7 MHz, D_2O), δ: 126.9 (C1, C15), 128.0 (C7, C9), 130.6 (C2, C14), 144.9 (C3, C13), 146.0 (C8), 151.6 (C4, C12), 152.2 (C5, C11), 156.7 (C6, C10) ppm. ^{195}Pt-NMR (107.2 MHz, D_2O), δ: 387 ppm. ESI-MS: calcd for $C_{15}H_{13}Cl_2N_3O_2Pt$ [M] 533 m/z, found (positive ion mode) 498 m/z $[M\text{-}Cl]^+$.

Synthesis of (*OC*-6-43)-(4-carboxypropanoato)chloridohydroxidoplatinum(IV) (3)

A solution of succinic anhydride (46.9 mg, 0.469 mmol) in 1 mL of DMF was added to a suspension of complex **2** (50.0 mg, 0.0938 mmol) in 2 mL of DMF and the reaction was carried out at 40 °C overnight. The solvent was then removed under reduced pressure and an orange solid was precipitated by the addition of acetone/diethyl ether. It was purified with an anionic exchange resin (Amberlite® IRA-400(OH) Supelco, in which the hydroxido groups were replaced by chloride anions) in order to remove free succinate and to introduce chlorides as counter ions. The resulting solution was dried under reduced pressure and the residue was washed with methanol and dried *in vacuo*. Yield: 44.8 mg, 0.0707 mmol, 75.4%. ^{1}H-NMR (500 MHz, D_2O), δ: 2.62 (s, H17, H18, 4H), 8.13 (m, H2, H14, 2H), 8.60 (t, H3, H13, 2H, ^3J = 7.9 Hz), 8.69 (d, H7, H9, 2H, ^3J = 7.9 Hz), 8.75 (s, H1, H8, H15, 3H), 9.34 (d, H4, H12, 2H, ^3J = 5.7 Hz) ppm. ^{13}C-NMR (125.7 MHz, D_2O), δ: 29.9 (C17, C18), 126.5 (C1, C15), 127.6 (C7, C9), 130.3 (C2, C14), 144.9 (C3, C13), 146.0 (C8), 151.7 (C4, C12), 152.8 (C5, C11), 157.3 (C6, C10), 177.2 (C19), 180.3 (C16) ppm. ^{195}Pt-NMR (107.2 MHz, D_2O), δ: 524 ppm. ESI-MS: calcd for $C_{19}H_{17}Cl_2N_3O_5Pt$ [M] 633 m/z, found (positive ion mode) 598 m/z $[M\text{-}Cl]^+$.

Loading of complex 3 on silica nanoparticles (conjugate 4)

A mixture of **3** (12.1 mg, 0.0191 mmol) and *N*-(3-dimethylaminopropyl)-*N'*-ethylcarbodiimide hydrochloride (EDC, 4.4 mg, 0.0229 mmol) in 1 ml of ultrapure water was magnetically stirred for 5 min at room temperature, then *N*-hydroxysuccinimide (NHS, 2.6 mg, 0.0229 mmol) was added and the reaction was performed for 30 min. In the meanwhile, an

ethanol suspension of amino-functionalized silica nanoparticles SNPs (13.67 mg mL^{-1}), prepared according to previously published procedures,[39] was centrifuged to remove the solvent, washed with ultrapure water, centrifuged and resuspended in water. The resulting suspension of SNPs was added to the previously prepared solution of activated **3** and the mixture was magnetically stirred for 2 h at room temperature to get conjugate **4**. The product was collected by centrifugation (10 min, 10000 rpm), washed several times with water and, then, resuspended in ethanol.

Quantification of the platinum content on conjugate 4

After microwave acid mineralization of conjugate **4**, the Pt content was determined by means of ICP-OES. In particular, the ethanol suspension of **4** was centrifuged to remove the alcohol and the solid portion was dried. Then, 2-3 mg of dry product were introduced into quartz cuvettes, together with 800 µL of 70% w/w HNO_3 and 200 µL of 35% w/w aqueous hydrogen peroxide. These devices were put into a closed vessel in the microwave oven (200 °C, 45 min, 1200 W microwave power). The vessel was then cooled to room temperature and the cuvettes were pulled out: their content was transferred into marked flasks using 1% v/v HNO_3 and sonicated for 1 h at 60 °C. After centrifugation (5 min, 10000 rpm) to remove the silica residue, the quantification of the Pt content of the supernatant was measured by ICP-OES. The results indicated a Pt loading of 6.23 µmol Pt g^{-1} NPs, corresponding to the conjugation of 2.2% of the total available amino groups (0.283 mmol NH_2 g^{-1} SNPs).

Stability and reactions in solution

The solution behavior of complexes **1** and **3** (0.5 mM) was studied in 2 mM HEPES buffer (HEPES = 4-(2-hydroxyethyl)-1-piperazineethanesulfonic acid, pH = 7.5) at 37 °C. The reduction of complex **3** (0.5 mM) with ascorbic acid (ascorbic acid:Pt molar ratio = 10:1) was studied in 2 mM HEPES at 37 °C. All these reactions were followed by monitoring the decrease of the area of the chromatographic peaks of the Pt complexes in HPLC-UV-MS and the increase of possible new peaks. The mobile phase was a mixture of 15 mM aqueous HCOOH and CH_3OH in ratios of 70/30 for **1** and 90/10 for **3**.

DFT calculations

All DFT calculations were carried out using Gaussian09[52] at the B3LYP[53, 54] level, using a basis set consisting of LANL2DZ on Pt[55, 56] and 6-31G(d)[57] on all remaining atoms. All species were fully optimized without any symmetry constraint, and confirmed as minima by harmonic frequency calculations. The same calculations were used to estimate thermal corrections to electronic energy to obtain enthalpy changes, and to extract HOMO/LUMO plots.

Cytotoxicity

Compounds **1**, **2** and **4** were tested on three cancer cell lines: the human ovarian carcinoma cell line A2780, purchased from ECACC (European Collection of Cell Cultures, UK), a primary malignant pleural mesothelioma (MPM) cancer cell line, derived of pleural effusion of previously untreated patients suffering from MPM, namely MM98 (sarcomatoid), and on a cisplatin-resistant cell line derived from wild type MM98 by exposure to sub-lethal concentrations of cisplatin for several months, called MM98R.[58] The last two cell lines were obtained from the Hospital of Alessandria (Pathology Unit).

A2780 were grown in RPMI1640, whereas DMEM (Sigma-Aldrich) was used for MPM cells. All media were supplemented with L-glutamine (2 mM), penicillin 100 IU mL^{-1}, streptomycin (100 mg L^{-1}) and 10% fetal bovine serum (FBS). Cell culture and the treatments were carried on at 37 °C in a 5% CO_2 humidified chamber. Cell were challenged with the compounds under study for 72 h continuous treatment (CT).

Cisplatin and complex **1** were dissolved in 0.9% w/v NaCl aqueous solution brought to pH 3 with HCl (final stock concentration 1 mM), complex **2** was dissolved in water (final stock concentration 5 mM), whereas conjugate **4** was suspended in absolute ethanol (final Pt stock concentration 0.125 mM). The mother solutions were diluted in complete medium to required concentration range. In the case of co-solvent the total absolute ethanol concentration never exceeded 0.2% (this concentration was found to be non-toxic to the cell tested).

To assess the growth inhibition of the compounds under investigation, a cell viability test, *i.e.* the resazurin reduction assay was used.[59] Briefly, cells were seeded in black sterile tissue-culture treated 96-well plates. At the end of the treatment, viability was assayed by 10 µg mL^{-1} resazurin (Acros Chemicals, France) in fresh medium for 1 h at 37 °C, and the amount of the reduced product, resorufin, was measured by means of fluorescence (excitation 535 nm, emission 595 nm) with a Tecan Infinite F200Pro plate reader (Tecan Austria). In each experiment, cells were challenged with the drug candidates at different concentrations and the final data were calculated from at least three replicates of the same experiment performed in triplicate. The fluorescence of 8 wells containing medium without cells were used as blank. Fluorescence data were normalized to 100% cell viability for non-treated cells. Half inhibiting concentration (IC_{50}), defined as the concentration of the drug reducing cell viability by 50%, was obtained from the dose-response sigmoid using Origin Pro (version 8, Microcal Software, Inc., Northampton, MA, USA).

Cellular uptake

Cells under investigation (2×10^6) were seeded in 25 cm^2 flasks and treated for 4 h with 10 µM of the complexes under investigation (1 µM in the case of **4**) in complete medium. After 4 h, cells were washed two times with PBS (1X), detached from the flask using 0.05% Trypsin 1X + 2% EDTA (HyClone, Thermo Fisher) and harvested in fresh complete medium. An automatic cell counting device (Countess®, Life Technologies), was used to measure the cell number and the mean diameter from every cell count. About 5×10^6 cells were transferred into a borosilicate glass tube and centrifugated at 1100 rpm for 5 min at room

temperature. The supernatant was carefully removed by aspiration; in order to limit the cellular loss, about 200 µL of the supernatant were left. Cellular pellets were stored at -80 °C until mineralization. After defrosting, 70% w/w HNO_3 was added and left 1 h at 60 °C in an ultrasonic bath. Before the measurement, the HNO_3 was diluted to a final 3% v/v concentration. Platinum determination was performed by inductively coupled plasma-mass spectrometry (ICP-MS, Thermo Optek X Series 2). Instrumental settings were optimized to yield maximum sensitivity for platinum. For quantitative determination, the most abundant isotopes of platinum and indium (used as internal standard) were measured at *m/z* 195 and 115, respectively.

The level of Pt found in cells after the treatment was normalized to the cell number and the cellular volume, calculated from the actual mean cell diameter measured for every sample, to obtain the intracellular Pt concentration. The ratio between the intracellular and the known extracellular concentration of offered Pt is defined accumulation ratio, AR.[60]

Conclusions

In summary, this research has shown that, differently from Pt(II) complexes containing aliphatic di- or triamines, the oxidation of Pt(terpy) compounds is much more difficult and leads to Pt(IV) complexes somewhat problematic to handle. In its intermediate form **2**, the Pt(IV)-terpy was reasonably easy to use in the functionalization of silica nanoparticles. Surprisingly, the cytotoxic features observed in similar Pt(IV)-SNPs conjugates were not repeated, despite increased cellular accumulation by endocytosis. The possible explanation of such unsatisfactory result may be traced back to the reactivity of the Pt(II) metabolite, obtained *in vitro* after reduction from **4**, with the free amino groups of the SNPs. However, the biological features of the conjugate **4** and that of the Pt(II)-terpy precursor **1** remain interesting in the case of cisplatin-resistant cell lines.

Acknowledgements

This research was supported by the Compagnia di San Paolo within the research project “Biplanes”. We were indebted to Inter-University Consortium for Research on the Chemistry of Metals in Biological Systems (CIRCMSB, Bari) for providing opportunities of stimulating discussion.

Notes and references

1. M. J. Cleare and J. D. Hoeschele, *Platinum Metals Review*, 1973, **17**, 2-13.
2. M. J. Cleare and J. D. Hoeschele, *Bioinorganic Chemistry*, 1973, **2**, 187-210.
3. M. J. Cleare, *Coordination Chemistry Reviews*, 1974, **12**, 349-405.
4. N. Farrell, Y. Qu, L. Feng and B. Van Houten, *Biochemistry*, 1990, **29**, 9522-9531.
5. L. S. Hollis, A. R. Amundsen and E. W. Stern, *Journal of Medicinal Chemistry*, 1989, **32**, 128-136.
6. L. S. Hollis, W. I. Sundquist, J. N. Burstyn, W. J. Heigerbernays, S. F. Bellon, K. J. Ahmed, A. R. Amundsen, E. W. Stern and S. J. Lippard, *Cancer Research*, 1991, **51**, 1866-1875.
7. K. S. Lovejoy, R. C. Todd, S. Z. Zhang, M. S. McCormick, J. A. D'Aquino, J. T. Reardon, A. Sancar, K. M. Giacomini and S. J. Lippard, *Proceedings of the National Academy of Sciences of the United States of America*, 2008, **105**, 8902-8907.
8. C. Francisco, S. Gama, F. Mendes, F. Marques, I. Cordeiro Dos Santos, A. Paulo, I. Santos, J. Coimbra, E. Gabano and M. Ravera, *Dalton Transactions*, 2011, **40**, 5781-5792.
9. G. Y. Park, J. J. Wilson, Y. Song and S. J. Lippard, *Proceedings of the National Academy of Sciences of the United States of America*, 2012, **109**, 11987-11992.
10. T. C. Johnstone, S. M. Alexander, W. Lin and S. J. Lippard, *Journal of the American Chemical Society*, 2014, **136**, 116-118.
11. M. T. Gregory, G. Y. Park, T. C. Johnstone, Y. S. Lee, W. Yang and S. J. Lippard, *Proceedings of the National Academy of Sciences of the United States of America*, 2014, **111**, 9133-9138.
12. M. W. Kellinger, G. Y. Park, J. Chong, S. J. Lippard and D. Wang, *Journal of the American Chemical Society*, 2013, **135**, 13054-13061.
13. T. C. Johnstone and S. J. Lippard, *Journal of the American Chemical Society*, 2014, **136**, 2126-2134.
14. T. C. Johnstone, G. Y. Park and S. J. Lippard, *Anticancer Research*, 2014, **34**, 471-476.
15. M. Ravera, E. Gabano, I. Zanellato, E. Perin, A. Arrais and D. Osella, *Bioinorganic Chemistry and Applications*, 2016.
16. S. X. Chong, S. C. F. Au-Yeung and K. K. W. To, *Current Medicinal Chemistry*, 2016, **23**, 1268-1285.
17. I. Eryazici, C. N. Moorefield and G. R. Newkome, *Chemical Reviews*, 2008, **108**, 1834-1895.
18. A. H. J. Wang, J. Nathans, G. van der Marel, J. H. van Boom and A. Rich, *Nature*, 1978, **276**, 471-474.
19. M. Howe-Grant and S. J. Lippard, *Biochemistry*, 1979, **18**, 5762-5769.
20. K. Suntharalingam, A. J. P. White and R. Vilar, *Inorganic Chemistry*, 2009, **48**, 9427-9435.
21. S. Bombard, M. B. Gariboldi, E. Monti, E. Gabano, L. Gaviglio, M. Ravera and D. Osella, *Journal of Biological Inorganic Chemistry*, 2010, **15**, 841-850.
22. C. Y. Wei, L. J. Ren and N. Gao, *International Journal of Biological Macromolecules*, 2013, **57**, 1-8.
23. E. Morel, F. Poyer, L. Vaslin, S. Bombard and M. P. Teulade-Fichou, *Inorganica Chimica Acta*, 2016, **452**, 152-158.
24. S. Gama, I. Rodrigues, F. Mendes, I. C. Santos, E. Gabano, B. Klejevskaja, J. Gonzalez-Garcia, M. Ravera, R. Vilar and A. Paulo, *Journal of Inorganic Biochemistry*, 2016, **160**, 275-286.
25. D. Colangelo and D. Osella, *Current Medicinal Chemistry*, 2005, **12**, 3091-3102.
26. D. Colangelo and D. Osella, *Journal*, 2009, **4**, 562-586.
27. G. Lowe, A. S. Droz, T. Vilaivan, G. W. Weaver, L. Tweedale, J. M. Pratt, P. Rock, V. Yardley and S. L. Croft, *Journal of Medicinal Chemistry*, 1999, **42**, 999-1006.
28. S. Bonse, J. M. Richards, S. A. Ross, G. Lowe and R. L. Krauth-Siegel, *Journal of Medicinal Chemistry*, 2000, **43**, 4812-4821.

29. V. M. Manikandamathavan, N. Duraipandy, M. S. Kiran, V. G. Vaidyanathan and B. U. Nair, *RSC Advances*, 2015, **5**, 24877-24885.
30. K. Mitra, A. Shettar, P. Kondaiah and A. R. Chakravarty, *Inorganic Chemistry*, 2016, **55**, 5612-5622.
31. Y. Shi, S. A. Liu, D. J. Kerwood, J. Goodisman and J. C. Dabrowiak, *Journal of Inorganic Biochemistry*, 2012, **107**, 6-14.
32. E. Wexselblatt and D. Gibson, *Journal of Inorganic Biochemistry*, 2012, **117**, 220-229.
33. D. Gibson, *Dalton Transactions*, 2016, **45**, 12983-12991.
34. T. C. Johnstone, K. Suntharalingam and S. J. Lippard, *Chemical Reviews*, 2016, **116**, 3436-3486.
35. G. T. Morgan and F. H. Burstall, *Journal of the Chemical Society*, 1934, 1498-1500.
36. F. G. Baddour, M. I. Kahn, J. A. Golen, A. L. Rheingold and L. H. Doerrer, *Chemical Communications*, 2010, **46**, 4968-4970.
37. T. Lammers, F. Kiessling, W. E. Hennink and G. Storm, *Journal of Controlled Release*, 2012, **161**, 175-187.
38. M. Ravera, E. Perin, E. Gabano, I. Zanellato, G. Panzarasa, K. Sparnacci, M. Laus and D. Osella, *Journal of Inorganic Biochemistry*, 2015, **151**, 132-142.
39. M. Ravera, E. Gabano, I. Zanellato, E. Perin, A. Arrais and D. Osella, *Dalton Transactions*, 2016, **45**, 17233-17240.
40. E. Gabano, S. Gama, F. Mendes, F. Fregonese, A. Paulo and M. Ravera, *Inorganica Chimica Acta*, 2015, **437**, 16-19.
41. J. X. McDermott, J. F. White and G. M. Whitesides, *Journal of the American Chemical Society*, 1976, **98**, 6521-6528.
42. G. Annibale and B. Pitteri, in *Inorganic Syntheses*, ed. J. R. Shaple, John Wiley & Sons, Inc., 2004, vol. 34, ch. 2, pp. 76-81.
43. P. Gramatica, E. Papa, M. Luini, E. Monti, M. B. Gariboldi, M. Ravera, E. Gabano, L. Gaviglio and D. Osella, *Journal of Biological Inorganic Chemistry*, 2010, **15**, 1157-1169.
44. G. Ermondi, G. Caron, M. Ravera, E. Gabano, S. Bianco, J. A. Platts and D. Osella, *Dalton Transactions*, 2013, **42**, 3482-3489.
45. M. Ravera, E. Gabano, G. Pelosi, F. Fregonese, S. Tinello and D. Osella, *Inorganic Chemistry*, 2014, **53**, 9326-9335.
46. G. Pelosi, M. Ravera, E. Gabano, F. Fregonese and D. Osella, *Chemical Communications*, 2015, **51**, 8051-8053.
47. M. Ravera, E. Gabano, I. Zanellato, F. Fregonese, G. Pelosi, J. A. Platts and D. Osella, *Dalton Transactions*, 2016, **45**, 5300-5309.
48. M. Ravera, E. Gabano, S. Tinello, I. Zanellato and D. Osella, *Journal of Inorganic Biochemistry*, 2017, **167**, 27-35.
49. S. R. A. Khan, S. Huang, S. Shamsuddin, S. Inutsuka, K. H. Whitmire, Z. H. Siddik and A. R. Khokhar, *Bioorganic & Medicinal Chemistry*, 2000, **8**, 515-521.
50. I. Zanellato, I. Bonarrigo, D. Colangelo, E. Gabano, M. Ravera, M. Alessio and D. Osella, *Journal of Inorganic Biochemistry*, 2014, **140**, 219-227.
51. M. Ravera, E. Gabano, I. Zanellato, I. Bonarrigo, M. Alessio, F. Arnesano, A. Galliani, G. Natile and D. Osella, *Journal of Inorganic Biochemistry*, 2015, **150**, 1-8.
52. M. J. Frisch, G. W. Trucks, H. B. Schlegel, G. E. Scuseria, M. A. Robb, J. R. Cheeseman, G. Scalmani, V. Barone, B. Mennucci, G. A. Petersson, H. Nakatsuji, M. Caricato, X. Li, H. P. Hratchian, A. F. Izmaylov, J. Bloino, G. Zheng, J. L. Sonnenberg, M. Hada, M. Ehara, K. Toyota, R. Fukuda, J. Hasegawa, M. Ishida, T. Nakajima, Y. Honda, O. Kitao, H. Nakai, T. Vreven, J. A. Montgomery Jr., J. E. Peralta, F. Ogliaro, M. J. Bearpark, J. Heyd, E. N. Brothers, K. N. Kudin, V. N. Staroverov, R. Kobayashi, J. Normand, K. Raghavachari, A. P. Rendell, J. C. Burant, S. S. Iyengar, J. Tomasi, M. Cossi, N. Rega, N. J. Millam, M. Klene, J. E. Knox, J. B. Cross, V. Bakken, C. Adamo, J. Jaramillo, R. Gomperts, R. E. Stratmann, O. Yazyev, A. J. Austin, R. Cammi, C. Pomelli, J. W. Ochterski, R. L. Martin, K. Morokuma, V. G. Zakrzewski, G. A. Voth, P. Salvador, J. J. Dannenberg, S. Dapprich, A. D. Daniels, Ö. Farkas, J. B. Foresman, J. V. Ortiz, J. Cioslowski and D. J. Fox, *Gaussian 09, Revision C.01,* Gaussian, Inc., Wallingford CT, 2010.
53. A. D. Becke, *Journal of Chemical Physics*, 1993, **98**, 5648-5652.
54. C. Lee, W. Yang and R. G. Parr, *Physical Review B*, 1988, **37**, 785-789.
55. R. Ditchfield, W. J. Hehre and J. A. Pople, *Journal of Chemical Physics*, 1971, **54**, 724-728.
56. P. C. Hariharan and J. A. Pople, *Theoretica Chimica Acta*, 1973, **28**, 213-222.
57. P. J. Hay and W. R. Wadt, *Journal of Chemical Physics*, 1985, **82**, 270-283.
58. I. Zanellato, C. D. Boidi, G. Lingua, P. G. Betta, S. Orecchia, E. Monti and D. Osella, *Cancer Chemotherapy and Pharmacology*, 2011, **67**, 265-273.
59. E. Magnani and E. Bettini, *Brain Research Protocols*, 2000, **5**, 266-272.
60. A. Ghezzi, M. Aceto, C. Cassino, E. Gabano and D. Osella, *Journal of Inorganic Biochemistry*, 2004, **98**, 73-78.